Int. J. Pure Appl. Sci. 9(1);115-126 (2023)

IJPAS
ijpas@munzur.edu.tr
ISSN: 2149-0910

Research article/Araştırma makalesi
DOI:10.29132/ijpas.1172085

Vibration Control of A Beam Under A Moving Mass Through Adjusting Trapezoidal Velocity Profile

Hira Karagülle[1], Murat Akdağ[2]*

[1]*Izmir University of Economics, Faculty of Engineering, Department of Mechatronic Engineering, İzmir, Türkiye*
[2]*Dokuz Eylül University, Faculty of Engineering, Department of Mechanical Engineering, İzmir, Türkiye*
hira.karagulle@gmail.com , murat.akdag@deu.edu.tr*
Received date:09.09.2022, Accepted date: 02.02.2023

Abstract

In this article, the residual vibration of a simply supported beam with a moving mass is studied. The mass moves from a starting point to an end point on the beam with a trapezoidal velocity profile having accelerating, constant velocity and decelerating time intervals. The residual vibration of the mid-point of the beam after the mass stops is analyzed. The mathematical model of the system is developed using the finite element (FE) theory. Newmark method is used for the solution of FE model having time dependent matrices because of the moving mass. The model is verified by comparing the solution results with the results given in the previous studies in the literature. It is seen that the relationship between the natural frequency of the system and the velocity profile of the moving mass has an effect on the residual vibration of the structure. If the natural frequency of the system and the inverse of the deceleration time interval of the moving mass are equal while the moving mass is at the stopping position, residual vibrations occur at a minimum level. It seen that with the right speed profile selection, the decrease in vibration levels approaches 70% during the movement and 80% after stopping.

Keywords: Moving mass, simply supported beam, vibration control, finite element analysis, Newmark method

Trapez Hız Profilinin Ayarlanması Yoluyla Hareketli Bir Kütle Altındaki Kirişin Titreşim Kontrolü

Öz

Bu makalede, hareketli bir kütleye sahip basit mesnetli bir kirişin artık titreşimi incelenmiştir. Kütle kiriş üzerinde başlangıç noktasından bitiş noktasına ivmelenen, sabit hız ve yavaşlayan zaman aralıklarına sahip trapez hız profili ile hareket etmektedir. Kütle durduktan sonra kirişin orta noktasının artık titreşimi analiz edilir. Sistemin matematiksel modeli, sonlu elemanlar (FE) teorisi kullanılarak geliştirilmiştir. Hareketli kütle nedeniyle zamana bağlı matrislere sahip FE modelinin çözümü için Newmark yöntemi kullanılmıştır. Model, çözüm sonuçları ile literatürde daha önce yapılan çalışmalarda verilen sonuçlar karşılaştırılarak doğrulanmıştır. Sistemin doğal frekansı ile hareket eden kütlenin hız profili arasındaki ilişkinin yapının artık titreşimi üzerinde etkili olduğu gözlemlenmiştir. Hareketli kütle durma konumunda iken sistemin doğal frekansı ile hareket eden kütlenin yavaşlama zaman aralığının tersi eşit ise artık titreşimler minimum seviyede oluşur. Doğru hız profili seçimi ile titreşim seviyelerindeki düşüşün hareket sırasında %70'e, durduktan sonra ise %80'e yaklaştığı gözlemlenmiştir.

Anahtar Kelimeler: Hareketli kütle, basit mesnetli kiriş, titreşim kontrolü, sonlu elemanlar analizi, Newmark yöntemi.

INTRODUCTION

Reducing vibrations in structures such as cranes and large-span cartesian robots is important for load positioning. The trend of lightening such structures has been increasing in recent years, but residual vibrations deteriorate the operational performance of such cranes and cartesian robots (Golovin, 2021).

The dynamic response and vibration control of structures with moving masses or loads has been an active research area since 1849 (Ryu and Kong, 2012). It has applications in the engineering systems like bridges, pipes, cranes, etc. There are a large number of articles published in this area. Here a

IJPAS
ijpas@munzur.edu.tr
ISSN: 2149-0910

Research article/Araştırma makalesi
DOI:10.29132/ijpas.1172085

summary of the review of the literature is given considering recent years.

Mohanty et al. (2019) proposed a nonlinear model to consider the coupling of beam and mass interaction for different boundary conditions. Ebrahimi-Mamaghani et al. (2020) investigated the forced and free vibration of axially graded Rayleigh and Bernoulli-Euler beams under moving load. Their model considered axial material gradation and rotary inertia factor. Dyniewicz et al. (2019) studied a nonlinear Gao beam under a moving mass or a massless point-force. They suggested that Bernoulli-Euler beam models may be used when the loads are small while Gao beam allows for moderate loads. Hamza et al. (2020) used the modeling language Modelica to study a simply supported beam under moving mass excitation. They proposed a vibration absorber attached to the moving mass to attenuate excessive vibrations.

Zhang et al. (2020) considered a periodically supported beam excited by a moving load and compared the results obtained by Bernoulli-Euler and Timoshenko beam formulations. They observed large differences for the analysis of parametric excitation. Dimitrovova (2017) gave the solution for the moving mass problem for finite and infinite beams on visco-elastic two-parameter foundation. They observed that in systems with damping, mass induced vibrations stopped over time. Assie et al. (2021) investigated the dynamic response of thick Timoshenko perforated beams under a moving load. They used equivalent bending stiffness depending on number of holes and the filling ratio which is defined as the ratio of material thickness between two holes to the period length. They analyzed the effect of perforation parameters on the dynamic behavior of beams.

Ryu and Kong (2012) investigated active vibration control of simply supported beams with a moving mass numerically and experimentally. They used Galerkin's mode summation method and fuzzy control. Seifoori et al. (2021) presented theoretical and experimental results on the dynamic response of thin rectangular plates subjected to moving mass. They used the classical plate theory and eigenfunction expansion theory. Rezaei and Porseifi (2018) used on-line neural network controller for vibration suppression of a simply supported beam under a moving mass. Ganjefar et al. (2015) used self-recurrent wavelet neural networks as an identifier and as a controller to suppress the vibration of a beam under a moving mass excitation. Zrnic et al (2013) considered the theoretical studies of moving loads on crane structures and discussed how to convert theoretical ideas into designing realistic mega quayside cranes. Foyuazat et al. (2018) studied the dynamics of a viscoelastic plate on a viscoelastic Winkler foundation with a moving mass on it.

Kiani (2017) studied the dynamic response of a functionally graded carbon nanotube reinforced composite cylindrical panel subjected to moving load on the panel surface. Frediani and Hosseini (2020) investigated the dynamic response of a simply supported relatively thick composite sandwich curved beam under a moving mass. They considered the rotary inertia and the transverse shear deformation.

Golovin and Palis (2020) presented a distributed parameter model of large gantry cranes. A nonlinear stabilizing control has been proposed to suppress horizontal oscillations excited by trolley motion. Golovin (2021) also studied various control strategies for vibration control in large gantry cranes. Golovin and Palis (2019) gave a robust controller design by the H_∞ loopshaping design procedure for active damping of gantry crane vibrations. They verified the procedure on a laboratory gantry crane experimentally. Xin et al. (2018) studied the structural vibration of ladle cranes. They considered cabin quality, position and structural damping of the main beam. They developed a mathematical model based on Lagrange's equation and verified the results with the results given by Esmailzadeh and Ghorashi (2007), and by Wu (2008).

There are studies on the passive vibration control of residual vibration in manipulators by input shaping. Ankaralı and Diken (1997) presented that the residual vibration of a single link driven by cycloidal rise motion can be suppressed for certain rise motion frequencies. Akdag and Sen (2021) considered shaping of S-curve velocity profiles. Shaping trapezoidal velocity profiles were considered theoretically and experimentally in the studies by Malgaca et al. (2016), Yavuz et al. (2016), and Karagulle et al. (2017) for a single link manipulator with a curved beam, for a single link composite manipulator, and for a two-link manipulator, respectively. It was observed that the selection of the deceleration time equals the first natural period suppresses the residual vibrations. Nguyen and Ngo (2016) developed three control algorithms based on

Int. J. Pure Appl. Sci. 9(1);115-126 (2023)

IJPAS
ijpas@munzur.edu.tr
ISSN: 2149-0910

Research article/Araştırma makalesi
DOI:10.29132/ijpas.1172085

input shaping method to suppress the residual vibration of a flexible beam. Li et. al.(2009) presented a low-vibration motion profile generation method to reduce the residual vibration. In the proposed motion profile, the acceleration profile is designed by using a level-shifted sinusoidal waveform to have an s-shape in order to control its change rate. Liu and Chen (2018) presented the new S-curve motion profile which are shaped by the continuous input shaper, that can greatly lower the vibration and shorten the settling time.

In this study, a simply supported beam with a moving mass is considered. The mass has a trapezoidal velocity profile which has three time intervals. These parts of the velocity profile are acceleration, constant velocity and deceleration. As the position of the moving mass changes, the natural frequency of the system also changes. The highest vibrations occur when the moving mass stops at the midpoint of the beam. Therefore, this position has been taken up. After the moving mass stopped, residual vibrations in the system are investigated. The effect of the relationship between the velocity profile of the moving mass and the natural frequency of the mass at stopping position on residual vibrations is researched in this study. It is seen that vibrations can be significantly reduced with the right velocity profile.

MATERIAL AND METHODS

Modelling By Using FE Theory

Obtaining FEM of the system

A MatLab code is developed and for this finite element analysis theory is based (Karagulle,2017). The system examined is shown in Fig 1. It is assumed that this system, located in the X-Y plane, makes lateral vibrations only in the Y direction. At points A and B at the ends of the beams, the freedom of rotation in the Z direction is open, and the freedom of rotation in the X and Y directions is closed. However, the effect of the weight of the car traveling in the system on the natural frequency of the rod is examined and there is no force component in the Z direction. Therefore, only lateral vibrations in the Y direction are considered. The beam is simply supported with a pin-joint at A and a roller at B. The length of the beam is L_{AB}. A moving mass, m, is located at C at the time t=0. The mass moves from C to D and it is located at D at the time $t=t_m$. The distances from A to C, from C to D, and from D to B are L_{AC}, L_{CD}, and L_{DB}, respectively. The origin of the Cartesian coordinates (x,y,z) is placed at A. The instantaneous travelling distance of the mass is s(t). The gravity ($g=9.81\ m/s^2$) is in the –y direction. The beam length, the starting and stopping positions of the moving mass are defined by the vector $q_P=[\ L_{AB}, L_{AC}, L_{AD}]$ in meters.

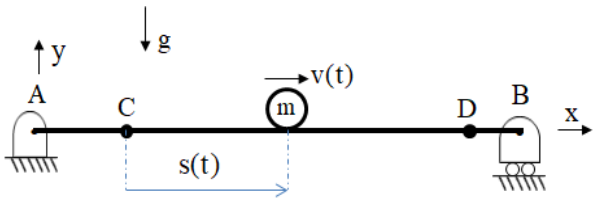

Figure 1. The system under study

The finite element model of the system is shown in Fig. 2.

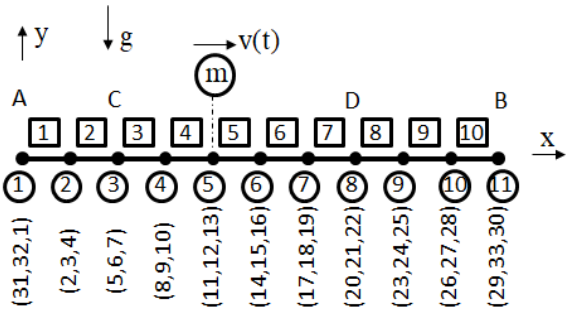

Figure 2. Finite element model

The numbers in the circles are the node numbers. The numbers in the squares are FE identification numbers. The analysis in the x-y plane is considered and each node has 3 degrees of freedom. The identification numbers of 3 displacements for each node are given in the parentheses. For example, FE-4 has Node-4 at its origin and Node-5 at the far end. The displacements for Node-5 are d_{s11}, d_{s12}, and, d_{s13} respectively. x_4, y_4 and z_4 are local Cartesian coordinates of FE-4. The local origin of FE-4 is at Node-4 and x_4 axis is towards Node-5. The planar motion is considered, and thus z_4 axis is always parallel to z axis. d_{s11} and d_{s12} are the displacements in the global x and y directions, respectively.

Int. J. Pure Appl. Sci. 9(1);115-126 (2023)

IJPAS
ijpas@munzur.edu.tr
ISSN: 2149-0910

Research article/Araştırma makalesi
DOI:10.29132/ijpas.1172085

$d_{s13}=h_4 r_{s13}$, where h_4 is the length of FE-4 and r_{s13} is the flexural rotation of the cross-section at Node-5. The number of finite elements is n_{fe}, and it is chosen as 10 in Fig. 2 for explanation. The model can be expanded with more finite element numbers.

The nodal displacements in the x and y directions, d_{s31} and d_{s32}, are zero for Node-1, because there is a pin. The nodal displacement in the y direction, d_{s33}, is zero for Node-11, because there is a roller. The degree of freedom of the system is $3n_{fe}$-3, which is 30 for n_{fe}=10. The index numbers of the constrained nodal displacements start with 31 for the example. Beam Finite Elements and their parameters are seen in Table 1.

Table 1. *Beam finite element model details and their parameters of the system*

FE-n	FE Nodes	Length	Orientation angle	Identification numbers for displacements at nodes
1	1,2	$h=L_{AB}/10$	0	31,32,1,2,3,4
2	2,3	h	0	2,3,4,5,6,7
3	3,4	h	0	5,6,7,8,9,10
4	4,5	h	0	8,9,10,11,12,13
5	5,6	h	0	11,12,13,14,15,16
6	6,7	h	0	14,15,16,17,18,19
7	7,8	h	0	17,18,19,20,21,22
8	8,9	h	0	20,21,22,23,24,25
9	9,10	h	0	23,24,25,26,27,28
10	10,11	h	0	26,27,28,29,31,30

Finite Element analysis theory is given in many textbooks. The displacement ($\mathbf{d_{eln}}$), stiffness ($\mathbf{k_{eln}}$), force ($\mathbf{f_{eln}}$), and mass ($\mathbf{m_{eln}}$) matrices in local coordinates of a finite element (FE-n) are given in Equation 1 and 2. The node numbers are j at the local origin, and k at the far end of FE-n. Flexural bending is about the z axis.

$$\mathbf{d}_{eln}=\begin{Bmatrix} u_{jn} \\ v_{jn} \\ h_n r_{jn} \\ u_{kn} \\ v_{kn} \\ h_n r_{kn} \end{Bmatrix} \quad \mathbf{k}_{eln}=\begin{bmatrix} \frac{AE}{h} & 0 & 0 & -\frac{AE}{h} & 0 & 0 \\ 0 & \frac{12EI}{h^3} & \frac{6EI}{h^2} & 0 & \frac{-12EI}{h^3} & \frac{6EI}{h^2} \\ 0 & \frac{6EI}{h^2} & \frac{4EI}{h} & 0 & \frac{-6EI}{h^2} & \frac{2EI}{h} \\ -\frac{AE}{h} & 0 & 0 & \frac{AE}{h} & 0 & 0 \\ 0 & \frac{-12EI}{h^3} & \frac{-6EI}{h^2} & 0 & \frac{12EI}{h^3} & \frac{-6EI}{h^2} \\ 0 & \frac{6EI}{h^2} & \frac{2EI}{h} & 0 & \frac{-6EI}{h^2} & \frac{4EI}{h} \end{bmatrix} \tag{1}$$

IJPAS
ijpas@munzur.edu.tr
ISSN: 2149-0910

Research article/Araştırma makalesi
DOI:10.29132/ijpas.1172085

$$\mathbf{f}_{eln}=\begin{Bmatrix} F_{jnx'}+q_{nx'}\frac{h_n}{2} \\ F_{jny'}+q_{ny'}\frac{h_n}{2} \\ T_{jn}+q_{ny'}\frac{h_n^2}{12} \\ F_{knx'}+q_{nx'}\frac{h_n}{2} \\ F_{kny'}+q_{ny'}\frac{h_n}{2} \\ T_{kn}+q_{ny'}\frac{h_n^2}{12} \end{Bmatrix} \quad \mathbf{m}_{eln}=\frac{\rho Ah}{420}\begin{bmatrix} 140 & 0 & 0 & 70 & 0 & 0 \\ 0 & 156 & 22h & 0 & 54 & -13h \\ 0 & 22h & 4h^2 & 0 & 13h & -3h^2 \\ 70 & 0 & 0 & 140 & 0 & 0 \\ 0 & 54 & 13h & 0 & 156 & -22h \\ 0 & -13h & -3h^2 & 0 & -22h & 4h^2 \end{bmatrix} \tag{2}$$

FE's with equal sizes and uniform cross-sectional areas are considered. The beam has homogeneous and isotropic material properties. L_{AB} is the length, A is the cross sectional area, and I is the cross sectional area moment of inertia of the beam. E is the modulus of elasticity, ρ is the density. u_{mn} is the nodal displacement at Node-m in the x_n direction, where m=j or k. v_{nm} is the nodal displacement in the y_n direction. r_{mn} is the flexural rotation of the cross section at Node-m. $F_{mnx'}$ and $F_{mny'}$ are the external load forces at Node-m in the x_n and y_n directions respectively. T_{mn} is the external bending moment at Node-m. $q_{nx'}$ and $q_{ny'}$ are the distributed external loads on the FE-n in the x_n and y_n directions, respectively.

The displacement ($\mathbf{d}_{egn}$) and stiffness ($\mathbf{k}_{egn}$), force ($\mathbf{f}_{egn}$), and mass ($\mathbf{m}_{egn}$) matrices of FE-n in global coordinates equal to $\mathbf{d}_{eln}$, $\mathbf{f}_{eln}$, $\mathbf{k}_{eln}$, and $\mathbf{m}_{eln}$, respectively, because the orientation of all the FE's are zero.

The mathematical model of the system is given below

$$\mathbf{m}_s\ddot{\mathbf{d}}_s+\mathbf{c}_s\dot{\mathbf{d}}_s+\mathbf{k}_s\mathbf{d}_s=\mathbf{f}_s$$

Here, $\mathbf{m}_s$, $\mathbf{c}_s$, $\mathbf{k}_s$, $\mathbf{d}_s$, $\mathbf{f}_s$ are respectively system mass matrix, system damping matrix, system stiffness matrix, system displacement matrix, system force matrix. The sizes of $\mathbf{d}_s$ and $\mathbf{f}_s$ are 30x1, and the sizes of $\mathbf{m}_s$, $\mathbf{c}_s$, and $\mathbf{k}_s$ are 30x30 for the configuration in Fig. 2. As examples, $\mathbf{d}_s(18,1)=d_{s18}$, which is the displacement of Node-7 in the y direction. $\mathbf{f}_s(15,1)=f_{s15}$, which is the external force at Node-6 in the y direction.

6x6 sized global matrices are assembled to create the system stiffness ($\mathbf{k}_s$) and the mass ($\mathbf{m}_s$) matrices. Such as,

$\mathbf{k}_s(15,14) = \mathbf{k}_{eg5}(5,4) + \mathbf{k}_{eg6}(2,1)$ and $\mathbf{m}_s(15,14) = \mathbf{m}_{eg5}(5,4) + \mathbf{m}_{eg6}(2,1)$

The combination of (15,14) exists in FE-5 and FE-6 as observed in Table-2.1. The combination of (15,14) is the combination of (5,4) for the FE-5 matrix, and the combination of (2,1) for FE-6 matrix.

The moving mass m, which is located at Node-5 instantaneously, is added to the system mass matrix as the following considering the kinetic energy.

$\mathbf{m}_s(11,11)=\mathbf{m}_{eg4}(4,4)+\mathbf{m}_{eg5}(1,1)+m$ and $\mathbf{m}_s(12,12)=\mathbf{m}_{eg4}(5,5)+\mathbf{m}_{eg5}(2,2)+m$

This addition is cancelled as the mass moves from Node-5 to Node-6 and revised as

$\mathbf{m}_s(14,14)=\mathbf{m}_{eg5}(4,4)+\mathbf{m}_{eg6}(1,1)+m$ and $\mathbf{m}_s(15,15)=\mathbf{m}_{eg5}(5,5)+\mathbf{m}_{eg6}(2,2)+m$

It is noted that the global mass matrix, $\mathbf{m}_s$, changes because of the moving mass, so it is time dependent.

Damping:

The Rayleigh damping is considered as

$$\mathbf{c}_s=\eta\mathbf{m}_s+\beta\mathbf{k}_s$$

where, η and β are damping coefficients (Thomson and Dahleh, 1988).

Motion:

The trapezoidal velocity profile of the mass is defined by the vector $q_V=[t_m,t_a,t_c,t_d,t_r]$ in seconds as shown in Fig. 3 (a). The residual vibration occurs at the time interval t_r after the mass stops at $t=t_m$. The integral of v(t) is the distance travelled by m and it is found as $L_{CD}=v_0(0.5t_a+t_c+0.5t_d)$.

Int. J. Pure Appl. Sci. 9(1);115-126 (2023)

IJPAS
ijpas@munzur.edu.tr
ISSN: 2149-0910

Research article/Araştırma makalesi
DOI:10.29132/ijpas.1172085

The travelling distance of the moving mass from one node to the adjacent node equals to the size of FE's, and given as $\Delta s=s_{i+1}-s_i=h=L_{AB}/n_{fe}$. Here i=1 to N, $N=n_{fe}+1$, $s_1=0$ and $s_N=L_{CD}$. The travelling time of the moving mass from one node to the adjacent node is $\Delta t_i=t_{i+1}-t_i$. Δt_i changes in the time intervals t_a and t_d. The following equations can be derived and are used calculate Δt_i.

$$t_i=\sqrt{\frac{2t_a s_i}{v_0}} \qquad v_i=\frac{v_0 t_i}{t_a} \qquad a_i=\frac{v_0}{t_a} \qquad \text{for } 0\le t<t_a$$

$$t_i=\frac{s_i-s_a}{v_0}+t_a \qquad v=v_0 \qquad a_i=0 \qquad \text{for } t_a\le t<t_M-t_d$$

$$\left.\begin{aligned} s_i&=\frac{-v_0(t_i-t_m+t_d)^2}{2t_d}+v_0(t_i-t_M+t_d)+v_0(t_M-t_d-t_a)+0.5v_0t_a \\ v_i&=-\frac{v_o(t_i-t_M+t_d)}{t_d}+v_0 \qquad a_i=-\frac{v_0}{t_d} \end{aligned}\right\} \text{for } t_M-t_d\le t<t_M$$

$$v_i=0 \qquad s_i=L_{CD} \qquad a_i=0 \qquad \Delta t_i=\Delta t_r \qquad \text{for } t_M\le t\le t_M+t_r$$

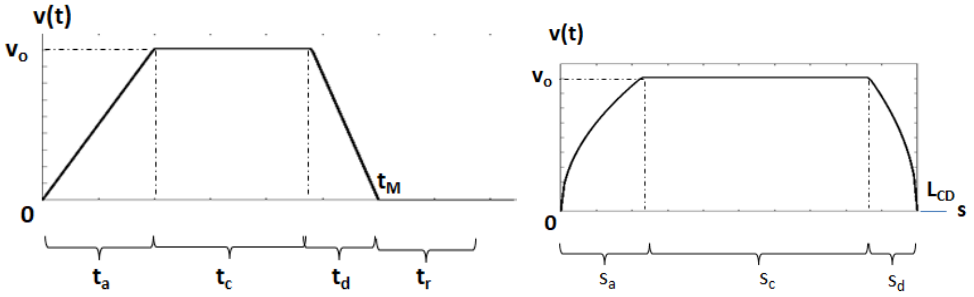

(a) (b)

Figure 3. Velocity profile a) with respect to time, b) with respect to travelling distance

Here, a_i is the acceleration of the moving mass at t_i. The FE size, $\Delta s=h$, determines Δt_i for $0\le t\le t_m$. $\Delta t_i=\Delta t_r$ is assigned freely considering the natural frequencies to analyze the residual vibration.

Forces:

There are gravity and inertia forces on the moving mass and distributed gravity forces on the beam. The distributed gravity force on FE-n is $q_{ny}=-\rho_n A_n g$, where $g=9.81$ m/s^2. For example, nodal forces for Node-7 are generated due to distributed forces for FE-6 and FE-7. So, the following can be written for the elements of the nodal force vector, $\mathbf{f}_s$, corresponding to Node-7.

$\mathbf{f}_s(18,1)=q_{6y}h_6/2+q_{7y}h_7/2$, and $\mathbf{f}_s(19,1)=q_{6y}h_6^2/12+q_{7y}h_7^2/12$.

The gravity and inertia forces of the moving mass are -mg in the y direction and $-ma_i$ in the x direction, respectively. These forces are added to the system force matrices as

$\mathbf{f}_s(12,1)=q_{4y}h_4/2+q_{5y}h_5/2-mg$, $\mathbf{f}_s(11,1)=-ma_3$, when the moving mass is located at Node-5.

These additions are cancelled when the moving mass moves from Node-5 to Node-6 and revised as

$\mathbf{f}_s(15,1)=q_{5y}h_5/2+q_{6y}h_6/2-mg$, $\mathbf{f}_s(14,1)=-ma_3$, when the moving mass is located at Node-6.

Vibration signals:

Let $d_{sensor}=\mathbf{d}_s(nsensor,1)$. The vibration in the y direction at the mid-point or at the stopping point is considered. n_{sensor} equals to 15 for the mid-point in the configuration in Fig. 2. n_{sensor} equals to 21 for the stopping-point at D in the configuration in Fig. 2. The second derivative of d_{sensor} is the acceleration signal and denoted by a_{sensor}.

Int. J. Pure Appl. Sci. 9(1);115-126 (2023)

IJPAS
ijpas@munzur.edu.tr
ISSN: 2149-0910

Research article/Araştırma makalesi
DOI:10.29132/ijpas.1172085

Modal Analysis

For this analysis, the following eigenvalue equation is solved.

$$\left|-\omega^2\mathbf{m}_s+\mathbf{k}_s\right|=0$$

ω is the un-damped natural frequencies of the system $\omega_1 T_1=2\pi$, where T_1 is the period corresponding the first natural frequency in seconds. $f_1=1/T_1$ is the first natural frequency in Hz. $\mathbf{m}_s$ changes because of the moving mass. Thus natural frequencies are changing depending on the position of the moving mass.

Newmark Method for Transient Analysis

The Newmark method (Newmark, 1959) is a numerical integration method used to solve differential equations and is used transient analysis. A time step, Δt, is chosen for the solution as $\Delta t<T_{max}/20$, where T_{max} is the period for the highest natural frequency considered. Knowing the solution at a time step, the solution at the subsequent time step is found by the numerical integration. t_i and t_{i+1} are the successive values for the time, and $\Delta t_{i+1}=t_{i+1}-t_i$. Let $\mathbf{m}_i$, $\mathbf{c}_i$, $\mathbf{k}_i$, $\mathbf{d}_i$, and $\mathbf{f}_i$ be the system mass, damping, stiffness, nodal displacement and nodal force matrices ($\mathbf{m}_s$, $\mathbf{c}_s$, $\mathbf{k}_s$, $\mathbf{d}_s$, and $\mathbf{f}_s$) at the time step t_i.

The Newmark solution is seen as

$$[a_0\mathbf{m}_{i+1}+a_1\mathbf{c}_{i+1}+\mathbf{k}_{i+1}]\mathbf{d}_{i+1}=\mathbf{f}_i+\mathbf{m}_i[a_0\mathbf{d}_i+a_2\dot{\mathbf{d}}_i+a_3\ddot{\mathbf{d}}_i]+\mathbf{c}_i[a_1\mathbf{d}_i+a_4\dot{\mathbf{d}}_i+a_5\ddot{\mathbf{d}}_I$$

$$\ddot{\mathbf{d}}_{i+1}=a_0[\mathbf{d}_{i+1}-\mathbf{d}_i]-a_2\dot{\mathbf{d}}_i-a_3\ddot{\mathbf{d}}_i \quad ,\dot{\mathbf{d}}_{i+1}=\dot{\mathbf{d}}_i+{}_a6\ddot{\mathbf{d}}_i+a_7\ddot{\mathbf{d}}_{i+1}$$

where

$$a_0=\frac{1}{\alpha\Delta t_{i+1}^2},a_1=\frac{\delta}{\alpha\Delta t_{i+1}},a_2=\frac{1}{\alpha\Delta t_{i+1}},a_3=\frac{1}{2\alpha}-1,a_4=\frac{\delta}{\alpha}-1$$

$$a_5=\frac{\Delta t_{i+1}}{2}\left(\frac{\delta}{\alpha}-2\right),a_6=\Delta t_{i+1}(1-\delta),a_7=\delta\Delta t_{i+1},\alpha=\frac{1}{4}(1+\gamma)^2$$

$$\delta=\frac{1}{2}+\gamma$$

γ is the amplitude decay factor, and it is taken as 0.005 in this study.

The flow chart of the MatLAB program which gives the samples of $\mathbf{d}_s$, $\dot{\mathbf{d}}_s$, and $\ddot{\mathbf{d}}_s$ is shown in Fig. 4.

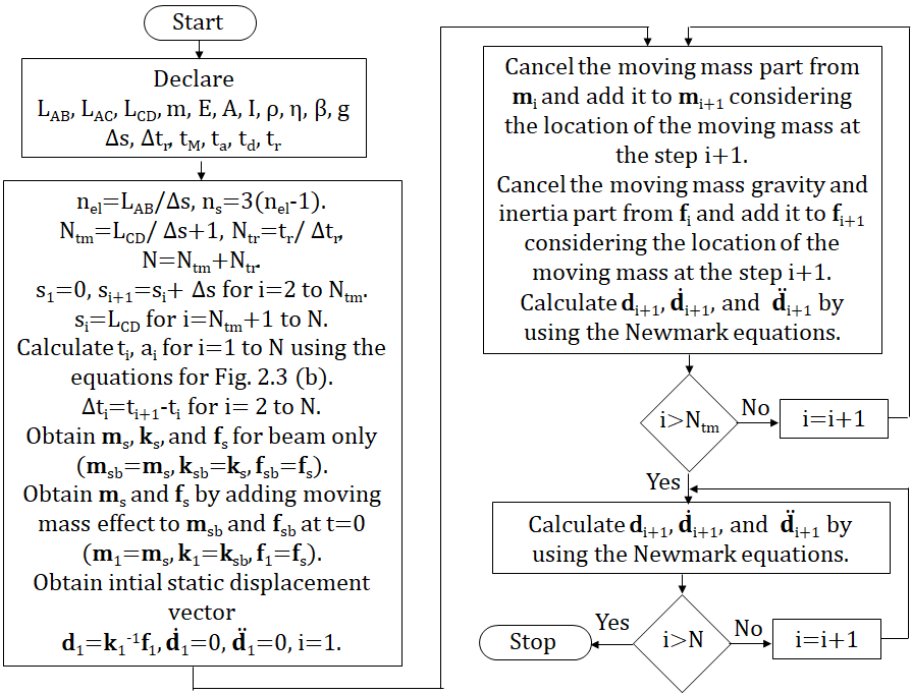

Figure 4. Flow chart of MatLAB program

VERIFYING FE MODEL

Example-1 is considered and simulation results are compared with the results given by Esmailzadeh and Ghorashi (1995), Xu et al. (2018), Wu (2008). The numerical values for the example are given as L_{AB}=10 m, $L_{AC}=L_{DB}$=0, m=70 kg, q_v=[3,0,0,0] s. Beam section dimensions: 0.007646 m x 0.11774 m. I=1.04 x 10^{-6} m^4. E=206.8 GPa, ρ=7820 kg/m^3.

Int. J. Pure Appl. Sci. 9(1);115-126 (2023)

IJPAS
ijpas@munzur.edu.tr
ISSN: 2149-0910

Research article/Araştırma makalesi
DOI:10.29132/ijpas.1172085

n_{el}=200. η=0, β=0. The result is shown in Fig. 5. The mid-point deflection value for t=0 is -20.9058 mm, and it is considered in the result. It is observed that the resulting response is in good agreement with the results given by Esmailzadeh and Ghorashi (1995), Xu et al. (2018), Wu (2008).

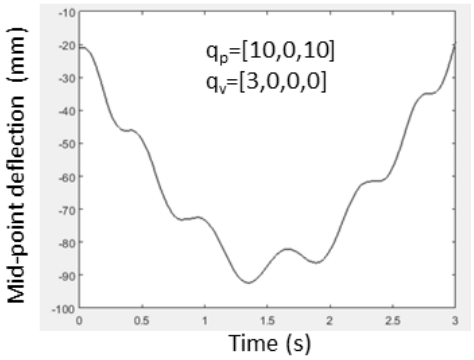

Figure 5. Mid-point deflection for Example-1

SIMULATION RESULTS AND DISCUSSIONS

Modal Analysis for Example-1

The change of the first natural frequency of the system for Example-1 depending on the location of the moving mass is shown in Fig. 6.

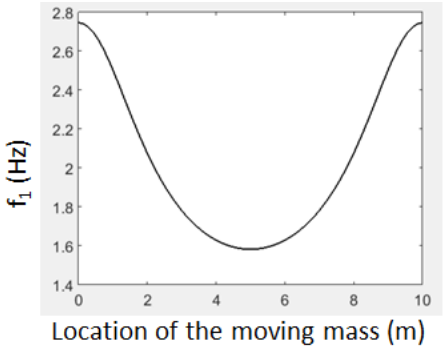

Figure 6. First natural frequency versus location of the moving mass

It is observed that the first natural frequency changes as 1.5830- 2.7455 Hz. It is minimum when the moving mass is located at the mid-point.

Analysis of effect of velocity profile for Example-1

The residual vibration and the effect of the velocity profile are studied in this section. This analysis is important for the structures like cranes. Various results are given in Fig. 7, 8 and 9 for different q_p and q_v.

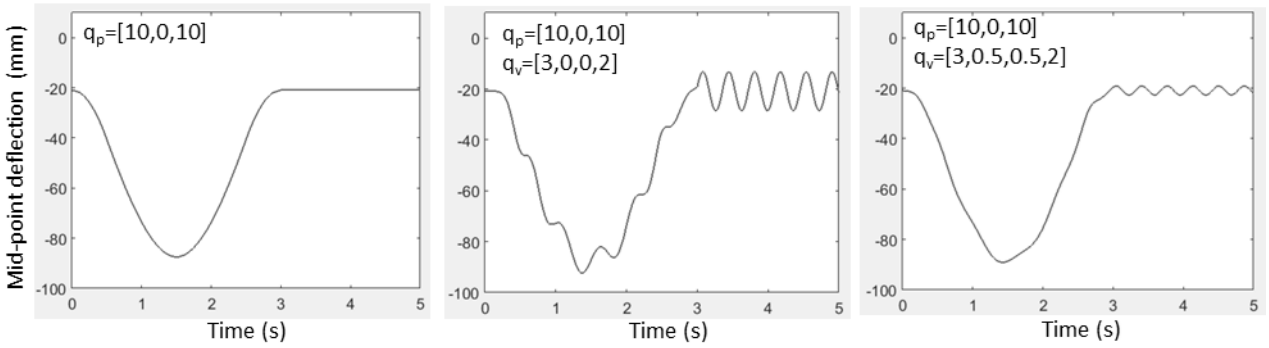

(a) (b) (c)

Figure 7. Mid-point deflections for (a) static solution, and (b) and (c) dynamic solutions for various velocity profiles

Int. J. Pure Appl. Sci. 9(1);115-126 (2023)

IJPAS
ijpas@munzur.edu.tr
ISSN: 2149-0910

Research article/Araştırma makalesi
DOI:10.29132/ijpas.1172085

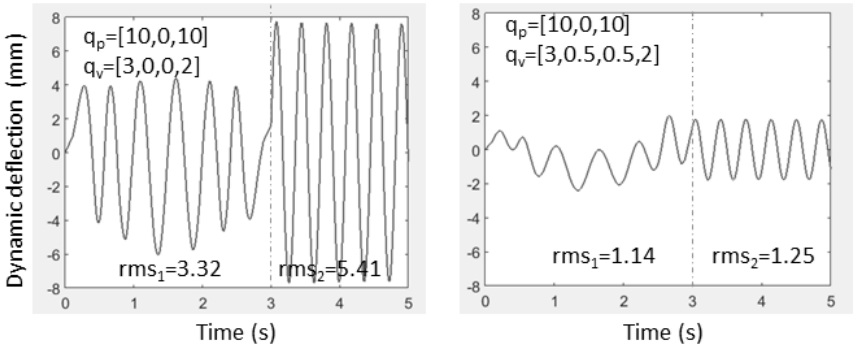

Figure 8. Mid-point dynamic deflections for solutions for various velocity profiles

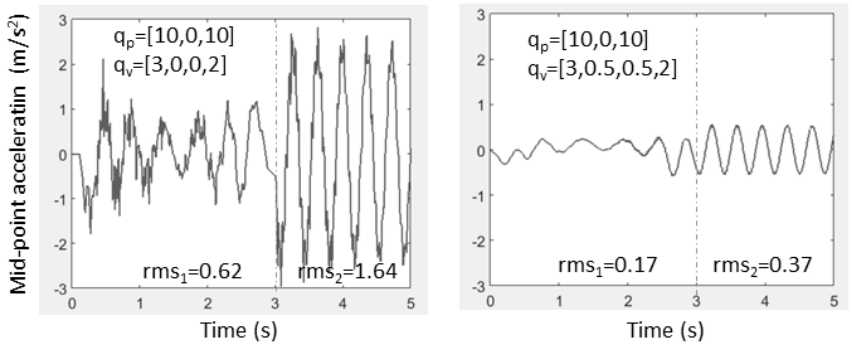

Figure 9. Mid-point accelerations for solutions for various velocity profiles

The deflection for the static solution in Fig. 7 (a) is subtracted from the deflections for the dynamic solutions in Fig. 7 (b) and (c) and the dynamic deflections shown in Fig. 8 are obtained. The midpoint accelerations are shown in Fig. 9. There are two regions in the results. Region-1 is for $0 \le t \le t_m$, and Region-2 for $t_m \le t \le t_m + t_r$. Region-1 is the time interval when the moving mass is in motion. Region-2 is the time interval for the residual vibration. Reducing the residual vibration is important in the systems like cranes. The vibration levels are evaluated by calculating the root mean square (rms) values. Let the rms values are rms_1 and rms_2 for the Region 1 and 2, respectively. The changes in the vibration levels are evaluated in Table 2.

The acceleration and deceleration times are changed from 0 to $0.5t_m$ with equal values (t_a=t_d). The changes of rms_1 and rms_2 values with respect to t_d are shown in Fig. 10 and 11 for different cases. The constant velocity for a case with t_d=0 is given as v_0=L_{CD}/t_m.

Table 2. *Vibration levels for the case q_p=[10,0,10]*

	q_v=[3,0,0,2]	q_v=[3,0.5,0.5,2]	Reduction[1]
Region-1/deflection	3.32	1.14	%66
Region-1/acceleration	0.62	0.17	% 68
Region-2/deflection	5.41	1.25	%77
Region-2/acceleration	1.64	0.37	%77

[1] *Reduction is calculated as 100(3.32-1.14)/3.32=66 for example*

Int. J. Pure Appl. Sci. 9(1);115-126 (2023)

IJPAS
ijpas@munzur.edu.tr
ISSN: 2149-0910

Research article/Araştırma makalesi
DOI:10.29132/ijpas.1172085

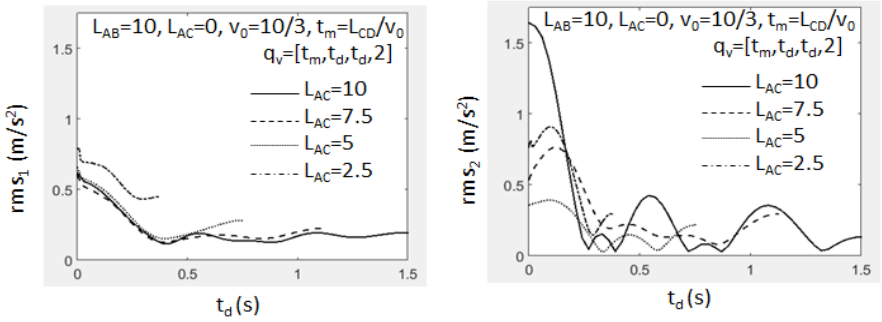

Figure 10. Change of rms values for different travelling distances with equal v_0

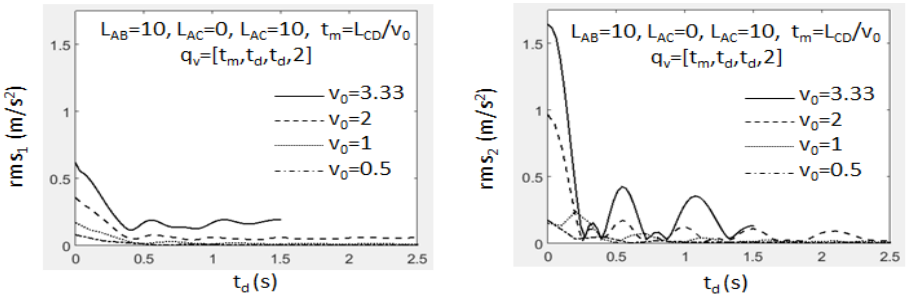

Figure 11. Change of rms values with respect to t_d for different travelling velocities

It is observed that the rms values depend on t_d. The vibration level in Region-2 is more sensitive to t_d. It is possible to reduce the residual vibration independent on the travelling distance and motion times.

The change of rms_2 values with respect to t_d for different lengths of beams are shown in Fig. 12. The moving mass starts from the point-A and stops at the mid-point. It is observed that the longer beam length the higher t_d at which the vibration levels reduce.

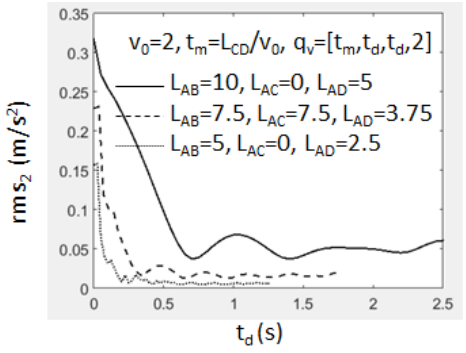

Figure 12. Change of rms_2 values with respect to t_d for different lengths of beams

Let f_{1m} be the first natural frequency for the system when the moving mass stops at the mid-point, and T_{1m}=1/f_{1m}. T_{1m} is the period in second determined by f_{1m}. f_{1m} equals to 1.58 Hz for L_{AB}=10 m, 2.55 Hz for L_{AB}=7.5 m, and 4.9 Hz for L_{AB}=5 m. f_{1m} increases as the length of the beam decreases, because the beam becomes more rigid. T_{1m} equals to 0.63 s for L_{AB}=10 m, 0.39s for L_{AB}=7.5 m, and 0.20 s for L_{AB}=5 m. It is observed from Fig. 12 that t_d values at which the vibration levels drop approximately equal to T_{1m}.

CONCLUSION

Dynamic analysis of beams with moving masses has been studied for many years and is still an active research area. It has applications in engineering structures such as trains, bridges, and cranes. There is a trend to design lighter structures with masses with higher speeds in recent decades. Faster cargo transportation demand requires less operation times. A lot of gantry cranes are operated at high velocities of crane trolleys. All these developments increased the studies on the vibration control of beams with moving masses.

There are studies on the passive vibration control of single links and two-link manipulators. It was

IJPAS
ijpas@munzur.edu.tr
ISSN: 2149-0910

Research article/Araştırma makalesi
DOI:10.29132/ijpas.1172085

observed that the shaping of velocity profiles results in the control of vibrations in these structures. The residual vibrations are suppressed if the deceleration time equals to the inverse of the first natural frequency of the structure. In this work, this approach is investigated for beams with moving masses. A finite element (FE) model is developed. The mass matrix of the FE model is time dependent because the mass is moving. The transient solutions are obtained by using Newmark method. Trapezoidal velocity profiles are considered where the mass strats the motion with a starting zero velocity, accelerates linearly in an acceleration time interval, continues its motion with a constant velocity with a constant velocity time interval, and then decelerates with a deceleration time interval and stops. The structure continues to vibrate after stopping, which is called as the residual vibration. Residual vibration levels have been found to be sensitive to deceleration times. The natural frequencies of the system are time dependent because of the moving mass. The vibration levels reduce significantly when inverse of the deceleration time equals to the first natural frequency of the system at the stopping position. According to the simulation results obtained, it is seen that not only residual vibrations but also vibration levels during movement decrease. Especially the decrease in residual vibration level approaches 80%.

Cranes, large cartesian robots carry variable loads during operation. The natural frequency of the system depends on both the size of the moving mass and its position on the system. Vibration levels can be kept at a minimum level if the velocity profile of the moving mass is made variable according to the defined work. The results of this study can be used in crane operations where to suppress the residual vibrations after stopping.

CONFLICT OF INTEREST

The Authors report no conflict of interest relevant to this article.

RESEARCH AND PUBLICATION ETHICS STATEMENT

The authors declare that this study complies with research and publication ethics.

REFERENCES

Akdağ M. and Şen H. (2021) S-curve motion profile design for vibration control of single link flexible manipulator. Dokuz Eylül Üniversitesi Mühendislik Fakültesi Fen ve Mühendislik Dergisi, 23(68), 661-676.

Ankaralı A. and Diken H. (1997) Vibration control of an elastic manipulator link. Journal of Sound and Vibration, 204(1), 162-170.

Assie A., Akbas S.D., Bashiri H.B., Abdelrahman A.A. and Eltaher M.A. (2021) Vibration response of perforated thick beam under moving load. Eurepean Physical Journal Plus, 136(283), 15 pages.

Dimitrovova Z. (2017) New semi-analytical solution for a uniformly moving mass on a beam on a two-parameter visco-elastic foundation. International Journal of Mechanical Sciences, 127, 142–162.

Dyniewicz B., Bajer C.A., Kuttler K.A. and Shillor M. (2019) Vibrations of a Gao beam subjected to a moving mass. Nonlinear Analysis: Real World Applications, 50, 342–364.

Ebrahimi-Mamaghani A., Sarparast H. and Masoud R. (2020) On the vibrations of axially graded Rayleigh beams under a moving load. Applied Mathematical Modelling, 84, 554–570.

Esmailzadeh E. and Ghorashi M. (1995) Vibration analysis of beams traversed by uniform partially distributed moving masses. Journal of Sound and Vibration, 184 (1), 9–17.

Foyouzat M.A., Estekanchi H.E. and Mofid M. (2018) An analytical-numerical solution to assess the dynamic response of viscoelastic plates to a moving mass. Applied Mathematical Modelling, 54, 670–696.

Freidani M. and Hosseini M. (2020) Elasto-dynamic response analysis of a curved composite sandwich beam subjected to the loading of a moving mass. Mechanics of Advanced Composite Structures, 7, 347–354.

Ganjefar S., Rezaei S. and Pourseifi M. (2015). Self-adaptive vibration control of simply supported beam under a moving mass using self-recurrent wavelet neural networks via adaptive learning rates. Meccanica, 50(12), 2879-2898.

Golovin I. (2021) Model-based control for active damping of crane structural vibrations. PhD Thesis, Fakultat fur Elektrotechnik und Informationstechnik der Otto-von-Guericke-Universitat, Magdeburg.

Golovin I. and Palis S. (2019) Robust control for active damping of elastic gantry crane vibrations. Mechanical Systems and Signal Processing, 121, 264–278

Golovin I. and Palis S. (2020) Modeling and discrepancy based control of underactuated large gantry cranes. IFAC PapersOnLine, 53(2),7783–7788

IJPAS
ijpas@munzur.edu.tr
ISSN: 2149-0910

Research article/Araştırma makalesi
DOI:10.29132/ijpas.1172085

Hamza G., Barkallah M., Hammadi M., Choley J. and Riviere A. (2020) Predesign of a flexible multibody system excited by moving load using a mechatronic system approach. Mechanics & Industry, 21(604), 9 pages.

Karagülle H., Malgaca L., Dirilmiş M., Akdağ M. and Yavuz Ş. (2017) Vibration control of a two-link flexible Manipulator. Journal of Vibration and Control, 23(12), 2023–2034.

Kiani Y. (2017) Dynamics of FG-CNT reinforced composite cylindrical panel subjected to moving load. Thin-Walled Structures, 111, 48–57

Li H., Le M.D., Gong Z.M., Lin W. (2009) Motion profile design to reduce residual vibration of high-speed positioning stages. IEEE/ASME Transactions On Mechatronics, 14(2),264-269

Liu C., Chen Y. (2018) Combined S-curve feedrate profiling and input shaping for glass substrate transfer robot vibration suppression. Industrial Robot: An International Journal 45/4, 549–560

Malgaca L., Yavuz Ş., Akdağ M. and Karagülle H. (2016) Residual vibration control of a single-link flexible curved manipulator. Simulation Modelling Practice and Theory, 67, 155-170.

Mohanty A., Varghese M.P. and Behera R.K. (2019) Coupled nonlinear behavior of beam with a moving mass. Applied Acoustics, 156, 367–377.

Newmark NM (1959) A method of computation for structural dynamics. Journal of Engineering Mechanics, ASCE 85, 67–94.

Nguyen Q.C., Ngo H.Q.T. (2016) Input shaping control to reduce residual vibration of a flexible beam. Journal of Computer Science and Cybernetics, 32(1), 73–88

Rezaei S. and Pourseifi M. (2018) vibration suppression of simply supported beam under a moving mass using on-line neural network controller. Journal of Solid Mechanics, 10(2),387-399.

Ryu B., and Kong Y. (2012) dynamic responses and active vibration control of beam structures under a travelling mass. In Advances on Analysis and Control of Vibrations-Theory and Applications, 231-252.

Seifoori S., Parrany A.H. and Darvishinia S. (2021) Experimental studies on the dynamic response of thin rectangular plates subjected to moving mass. Journal of Vibration and Control 27(5-6), 685-697.

Thomson W.T. and Dahleh M.D. (1988) Theory of vibration with applications, (3rd edition). Englewood Cliffs: Prentice-Hall.

Xin Y., Xu G., Su N. and Dong Q. (2018) Nonlinear vibration of ladle crane due to a moving trolley. Hindawi Mathematical Problems in Engineering, 4, 1-14 pages.

Wu J.J. (2008) Transverse and longitudinal vibrations of a frame structure due to a moving trolley and the hoisted object using moving finite element. International Journal of Mechanical Sciences 50 (4), 613–625.

Yavuz Ş., Malgaca L. and Karagülle H. (2016) Vibration control of a single-link flexible composite manipulator. Composite Structures , 140, 684-691

Zhang X., Thompson D. and Sheng X. (2020) Differences between Euler-Bernoulli and Timoshenko beam formulations for calculating the effects of moving loads on a periodically supported beam. Journal of Sound and Vibration 481 (115432), 14 pages.

Zrnic N., Gasic V., Bosnjak S. and Dordevic M. (2013). Moving loads in structural dynamics of cranes: bridging the gap between theoretical and practical researches. FME Transactions 41(4), 291-297.